ENDOR Determined Structure of a Complex of α-Chymotrypsin with a Spin-Labeled Transition-State Inhibitor Analogue

Fashun Jiang, Shih-Wa Tsai, Shan Chen, and Marvin W. Makinen*

Department of Biochemistry and Molecular Biology, The University of Chicago, Cummings Life Science Center, 920 E. 58th Street, Chicago, Illinois 60637

Received: August 22, 1997; In Final Form: March 3, 1998

The conformation of the spin-labeled compound *N*-(2,2,5,5-tetramethyl-1-oxypyrrolinyl-3-carboxyl)-L-phenylalaninal (SLPheal), synthesized as a transition-state inhibitor analogue of α-chymotrypsin (αCT), has been determined by electron nuclear double resonance (ENDOR) and molecular modeling methods for both the free inhibitor in solution and the hemiacetal enzyme:inhibitor adduct. SLPheal exhibited linear, competitive inhibition of αCT with $K_I = (0.21 \pm 0.03) \times 10^{-3}$ M. By a combination of NMR and ENDOR spectroscopy, we have established that 92% of the aldehyde is found as the hydrated aldehyde species $RCH(OH)_2$ at pH 7.0. From ENDOR spectra, principal hyperfine coupling (hfc) components of specific protons assigned by selective deuteration were determined, and their corresponding dipolar hfc components were computed to estimate electron−proton distances. The principal hfc components of the fluorine substituent of a ζF-phenylalaninal inhibitor analogue were also determined for estimation of electron−fluorine distances. With these ENDOR determined distances as constraints, the conformation of the inhibitor both free in solution and in the active site of αCT was determined on the basis of torsion angle search calculations and molecular graphics analysis. Comparison of the conformation of the inhibitor free in solution and bound to αCT showed that formation of the hemiacetal enzyme:inhibitor adduct required positioning of the spin-label group with torsional alteration in inhibitor structure similar to that described for the spin-labeled tryptophanyl moiety in an acylenzyme reaction intermediate of αCT [Wells et al., *J. Biol. Chem.* **1994**, *269*, 4577−4586]. While the ENDOR results of the hemiacetal formed in neat methanol were distinguishably different for *R* and *S* configurations modeled for an sp^3 hybridized C atom of the aldehyde functional group, only an *S* configuration in the enzyme:inhibitor adduct was compatible with all of the ENDOR constraints. Since the inhibitor in aqueous solution is found largely in its hydrated form, it is probable that this is the predominant species that is initially bound in the active site of the enzyme. Accordingly, a reaction scheme is suggested for dehydration of the active site bound diol species catalyzed by the protonated form of His-57 to allow formation of the hemiacetal adduct with the side chain of Ser-195 having only an *S* configuration.

Introduction

The catalytic mechanism of α-chymotrypsin (EC 3.4.21.1), the leading member of a family of homologous enzymes known as the serine proteases, involves formation of two tetrahedral transition-state species through which the substrate becomes covalently linked to the side-chain of Ser-195 to form a metastable acylenzyme intermediate followed by breakdown to form reaction products.[1−5] While the tetrahedral species are not stable, compounds that mimic or form tetrahedral adducts with the side chain of Ser-195 have been employed as transition-state inhibitor analogues of the enzyme.[6,7] In particular, aldehydes form hemiacetal adducts, and evidence for hemiacetal formation with the side chain of Ser-195 in the active site of α-chymotrypsin has been reported by cross-saturation nuclear magnetic resonance studies for *N*-acyl-L-phenylalaninals,[7a] hydrocinnamaldehyde,[7b] and the dipeptide aldehyde *N*-trifluoroacetyl-L-phenylalaninal.[7c] No adduct of α-chymotrypsin with an aldehyde has been structurally characterized by X-ray diffraction, and conformational analysis of hemiacetal adducts of α-chymotrypsin in solution has been carried out only for aldehyde inhibitors with chiral centers remote from the catalytic site.[8] However, the X-ray structure of a hemiacetal adduct has been determined for protease A of *Streptomyces griseus* with chymostatin, a naturally occurring serine protease inhibitor that contains a C-terminal L-phenylalaninal residue.[9] In the adduct formed with this inhibitor, both *R* and *S* configurations of the hemiacetal are observed in equal populations.[9b]

We have shown that electron nuclear double resonance (ENDOR[10]) spectroscopy of nitroxyl spin-labels in solution can be incisively applied to determine structure and conformation with an accuracy exceeded only by that of single-crystal X-ray diffraction methods.[11−13] Here we describe the ENDOR-determined structure of the hemiacetal adduct of α-chymotrypsin formed with the synthetic, spin-labeled inhibitor *N*-(2,2,5,5-tetramethyl-1-oxypyrrolinyl-3-carboxyl)-L-phenylalaninal (SLPheal[10]). ENDOR spectroscopy was employed to determine the dipolar separations between the unpaired electron of the nitroxyl group[11e] and surrounding nuclei for use as constraints in torsion angle search calculations to assign the conformation of the inhibitor free in solution and in the active site of the enzyme. We found that the active site of the enzyme restricts the hemiacetal adduct to an *S* configuration while the ENDOR data for the chemically analogous adduct of the free inhibitor formed

* To whom correspondence should be addressed: Tel 773/702-1080; FAX 773/702-0439; E-mail m-makinen@uchicago.edu.

S1089-5647(97)02742-9 CCC: $15.00
Published on Web 05/12/1998

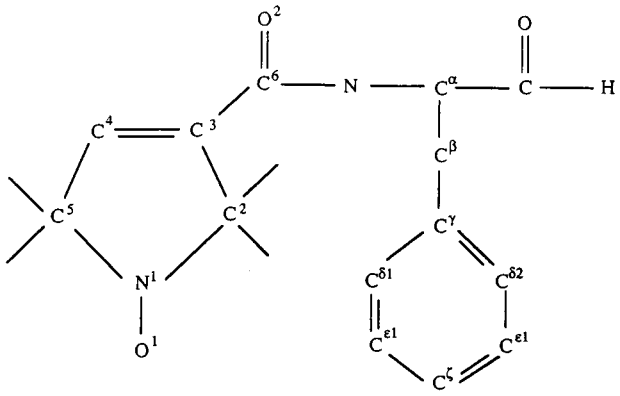

I SL *L*-phenylalaninal

II SL *L*-(α-^{2}H)phenylalaninal

III SL *L*-(δ1, δ2, ε1, ε2, ζ-$^2H_5$)-phenylalaninal

IV SL *L*-(β1, β2, δ1, δ2, ε1, ε2, ζ-$^2H_7$)-phenylalaninal

V SL *L*-(ζ-F)-phenylalaninal

Figure 1. Illustration of the chemical bonding structure and the atomic numbering scheme of specifically deuterated and fluorinated analogues of *N*-(2,2,5,5-tetramethyl-1-oxypyrrolinyl-3-carboxyl)-L-phenylalaninal used in this investigation. SL refers to the spin-label acyl moiety attached to the amino nitrogen atom.

in neat methanol show the presence of both *R* and *S* configurations. Since the hydrated form of the aldehyde inhibitor can be sterically accommodated in the active site, these results suggest that a catalytic residue in the active site, namely His-57, must facilitate dehydration of the diol species upon binding in the active site to allow subsequent adduct formation with the side chain of Ser-195.

Experimental Procedures

Materials. *General.* αCT[10] was obtained from Worthington Biochemical Co. (Freehold, NJ) as a thrice crystallized powder. Methyl *N*-(2,2,5,5-tetramethyl-1-oxypyrrolinyl-3-carboxyl)-L-phenylalanate and specifically deuterated and fluorinated analogues were prepared in conjunction with earlier studies.[11d] Diisobutylaluminum hydride was obtained from Aldrich Chemical Co. (Milwaukee, WI). Deionized, distilled water was used throughout.

N-(2,2,5,5-Tetramethyl-1-oxypyrrolinyl-3-carboxyl)-L-*phenylalaninal (SLPheal).* The series of natural abundance, fluorinated, and site-specific deuterium-enriched analogues of spin-labeled L-phenylalaninal (**I**−**V**) employed in this investigation is illustrated in Figure 1. We describe below the synthesis of **I**. This procedure was followed also for the deuterated and fluorinated analogues **II**−**V** illustrated in Figure 1. All synthetic products were confirmed by elemental analysis, mass spectrometry, and melting point determination.

Synthesis of **I** was developed following the method of Ito et al.[14] *N*-(2,2,5,5-Tetramethyl-1-oxypyrrolinyl-3-carboxyl)-L-phenylalanate[11d] (1.8 g, 5.2 mmol) was dissolved in dry dimethyloxyethane (35 mL) and cooled to −60 °C in a dry ice/chloroform bath. A solution of diisobutylaluminum hydride (12.5 mL, 1.0 M in toluene) was added dropwise under rapid stirring over a period of 15 min in a stream of dry nitrogen. The reaction mixture was kept at −60 °C for 75 min further before addition of a solution of citric acid (7 g, 3.27 mmol) in 50 mL of water and gradual warming of the mixture to room temperature. The mixture was extracted with ethyl acetate; the extracts were washed with water, filtered, and concentrated by rotary evaporation. The product was redissolved in 75 mL of methanol/water (60:40 v/v), and $NaHSO_3$ (2.70 g, 25.9 mmol) was added. After ca. 3.5 h the methanol was removed by rotary evaporation, 50 mL of water was added, and the mixture was extracted with ethyl acetate. The pH of the aqueous mixture was then adjusted to 9.5 with solid Na_2CO_3, and the aldehyde was extracted with ethyl acetate. The ethyl acetate extracts were combined, washed with water, and concentrated by rotary evaporation, the resultant oil was dissolved in 90 mL of methanol/water (60:40 v/v), and impurities were further removed by extraction with 5 × 25 mL of diethyl ether/hexanes (1:1 v/v). After removing methanol again by rotary evaporation and adding 40 mL of water, the aldehyde was extracted into ethyl acetate and dried over $MgSO_4$. Crystallization from tetrahydrofuran/methanol (1:1 v/v) and pentane produced a yellow crystalline solid (0.26 g, 14% yield, mp 91−92 °C). Elemental analysis was not consistent with that expected for the pure aldehyde ($C_{18}H_{23}O_3N_2$) but rather indicated that SLPheal crystallized with the equivalent of one tightly bound methanol molecule which we presumed to have formed an adduct with the aldehyde product ($C_{19}H_{27}O_4N_2$ theoretical/experimental: C, 65.68/65.26; H, 7.83/7.76; N, 8.06/7.84; O, 18.42/18.39). This was subsequently confirmed by fast atom bombardment mass spectrometry while electron impact mass spectrometry as a higher energy methodology showed only that the highest molecular ion peak corresponded to the free aldehyde.

To confirm the analytical results indicating that SLPheal was obtained as an RCHO:CH_3OH or RCH(OH)(OCH_3) hemiacetal adduct, the crystalline product was dissolved in ^2H_2O/[$^2H_6$]-DMSO (92:8 v/v) and kept for 1 day at 4 °C. The solution was lyophilized, and the dried compound was dissolved in ^2H_2O containing 8% (v/v) [$^2H_6$]DMSO and buffered to pD 7.0 with 0.05 M Na_3PO_4 and 1.0 M NaCl. On the basis of the chemical shift of the aldehydic proton at 9.67 ppm, the hydration constant[7a] K_H ([RCH(OH)$_2$]/[RCHO]) of SLPheal was found to be 11.0. In a solution of 75% (v/v) [$^2H_6$]DMSO, the value of K_H was reduced to 2.1. On this basis we estimate that, in a solution of 8% (v/v) DMSO buffered to pH or pD 7.0, at least 92% of the SLPheal exists as the hydrated RCH(OH)$_2$ species.

Methods. *Enzyme Kinetics.* The inhibitor (dissociation) constant K_I of SLPheal binding to αCT was determined by steady-state kinetic measurements. Initial velocity data for the hydrolysis of methyl *N*-acetyl L-tryptophanate in the presence of different concentrations of SLPheal were obtained by monitoring the change in absorbance at 300 nm with a Cary 15 spectrometer modified by On-Line Instrument Systems, Inc. (Jefferson, GA) for microprocessor-controlled data acquisition. A vibrating reed stirring assembly was employed for collection of kinetic data.[15] The hydrolysis-induced change in molar absorptivity ($\Delta\epsilon_{300}$) of 311 M^{-1} cm^{-1} was used for calculation of kinetic parameters.[12a,16] The values of the steady-state kinetic parameters K_M and k_{cat} were estimated with use of the iterative, nonlinear, least-squares fitting program ENZKIN provided by Professor J. Westley (Department of Biochemistry and Molecular Biology, The University of Chicago), as previously described.[12a,17] The inhibitor binding constant K_I was estimated from a plot of the slope of V_{max}/K_M vs [I].[18]

EPR and ENDOR. An X-band Bruker ESP 300E spectrometer equipped with a TM_{110} cylindrical cavity, Bruker ENDOR accessory, and Oxford Instruments ESR910 liquid helium cryostat was used for spectral data collection as previously described.[11,12,19] Typical experimental conditions for ENDOR

measurements were as follows: sample temperature, 40 K; microwave power, 0.52 mW; rf power, 50 W; rf modulation depth, 8−10 kHz. The static laboratory magnetic field was not modulated for ENDOR.

For ENDOR of free SLPheal, the aldehyde was first dissolved in pure [$^2H_6$]DMSO, and the mixture was than added to a solution of 1.0 M NaCl in ^2H_2O buffered to pD 7.0 with 0.01 M sodium cacodylate and lyophilized. This procedure was repeated twice. The final concentration of the free SLPheal in EPR sample tubes was 3×10^{-3} M in a solvent mixture of ^2H_2O/[$^2H_6$]DMSO (92:8 v/v). We also compared the ENDOR spectra of the solutions of SLPheal prepared as described above at pD 7.0 to those obtained for the adduct formed in neat [$^2H_1$]-methanol, [$^2H_3$]methanol, or [$^2H_4$]methanol.

For ENDOR spectroscopy of the enzyme adduct, the inhibitor was first dissolved in [$^2H_6$]DMSO and diluted by adding sodium cacodylate buffer at pD 7.0 to 60% [$^2H_6$]DMSO (v/v), incubating the mixture at room temperature for 1 h in order to allow isotopic exchange of the amide proton, and cooling to 0 °C. The enzyme was dialyzed against 0.1 M NaCl buffered to pD 4.7 with 0.05 M sodium [$^2H_3$]acetate to remove exchangeable protons. Sodium cacodylate was then added to the αCT solution, the pD was adjusted to 7.0, and the temperature was maintained at 20 °C for 10 min. An aliquot of the inhibitor solution was mixed with the αCT solution and incubated at 0 °C for 10 min and then frozen in liquid nitrogen for ENDOR data collection. Typical final concentrations of inhibitor and enzyme in ENDOR samples were 1.47×10^{-3} and 4.3×10^{-3} M, respectively, in a solvent mixture of ^2H_2O/ [$^2H_6$]DMSO (92:8 v/v) containing 0.1 M NaCl at pD 7.0.

Molecular Modeling. Atomic coordinates of non-hydrogen atoms of **I** were derived from the coordinates of methyl *N*-(2,2,5,5-tetramethyl-1-oxypyrrolinyl-3-carboxyl)-L-phenylalanate employed in earlier studies.[11d] Positions of hydrogen atoms were calculated for idealized geometries with C−H bond lengths of 1.08 and 1.045 Å for sp^3 and sp^2 hybridized carbons, respectively, and an N−H bond length of 1.00 Å. Coordinates of αCT were those of the tosyl derivative of αCT[4d] and were obtained from the Brookhaven Protein Data Bank (File 2CHA). As we have previously described,[11e] the position of the effective dipole of the unpaired electron, located 0.569 Å from the nitroxyl nitrogen atom along the N−O bond, was applied as the reference position within the molecular framework of the spin-label group.

Molecular modeling was carried out with the programs FRODO,[20a] INSIGHT,[20b] and SYBYL[20c,d] running on an Evans & Sutherland PS390 graphics terminal with a host VAX3500 computer, as previously described.[11,12] The nonbonded parameters described by Iijima et al.[21] were employed for torsional angle search calculations which were carried out with SEARCH within the SYBYL program package. ENDOR determined electron−nucleus distances, including their respective line width based uncertainties, were used as constraints in the search calculations. The basic philosophy and elements underlying the use of this program package have been described by Naruto et al.[22] and by us[11−13] previously.

Results

Inhibition of αCT by SLPheal. SLPheal exhibited simple, linear, competitive inhibition against the αCT catalyzed hydrolysis of methyl *N*-acetyl-L-tryptophanate, yielding a value for K_I of $(0.21 \pm 0.03) \times 10^{-3}$ M. This value is comparable to that of 0.7×10^{-3} M determined for *N*-acetyl-L-phenylalaninal[7a] and is consistent with inhibitor constants determined for other similar *N*-acyl-L-phenylalaninals.[7a,23] The inhibitor constant was determined from buffer solutions containing 3% methanol to avoid the added (competitive) inhibitory effect of DMSO on the enzyme while the ENDOR spectra were taken of samples in buffer solutions containing 8% DMSO. We have observed no difference in the ENDOR spectra of SLPheal in solutions containing 8% [$^2H_6$]DMSO or 6% [$^2H_4$]methanol in 0.1 M NaCl buffered to pD 7.0 with 0.01 M sodium cacodylate and conclude that this difference in solvent systems does not influence the intrinsic binding properties of the inhibitor to the enzyme. Correspondingly, for 4.3×10^{-3} M αCT and 1.47×10^{-3} M SLPheal, as typical concentrations employed for ENDOR studies, more than 91% of the SLPheal is calculated to be bound by the enzyme according to the value of K_I determined kinetically. Under these conditions of enzyme and inhibitor concentrations, the ENDOR signals detected are dominated by the hemiacetal enzyme:inhibitor adduct.

Analysis of ENDOR Spectra and Estimation of Electron−Nucleus Distances. *Free Inhibitor in Solution.* We have previously outlined the stratagem of employing the EPR characteristics of nitroxyl spin-labels for selection of molecular orientation in ENDOR studies.[11−13] For nitroxyl spin-labels in frozen solutions, the plane of the oxypyrrolinyl ring of molecules contributing to resonance is oriented perpendicularly to $\mathbf{H}_0$ when the static laboratory magnetic field is set to the low-field feature of the EPR spectrum (termed *setting A*), whereas essentially all orientations are selected when the magnetic field is set to the central resonance absorption feature of the EPR spectrum (termed *setting B*).

Figure 2 shows proton ENDOR spectra of the solvated aldehyde of **IV** in two different solutions. For the upper spectrum, the sample was prepared in such a way that crystalline SLPheal was first dissolved in a small volume of [$^2H_6$]DMSO. To the mixture was then added [$^2H_4$]methanol with rapid mixing and freezing in liquid nitrogen to minimize exchange of the amide proton. The parallel hfc features of H^N are easily recognized on the basis of our studies of derivatives of spin-labeled amino acids[11b−d] while the perpendicular hfc features are seen to overlap with the parallel hfc features of H^α. The perpendicular hfc feature of H^N was observed in the proton ENDOR spectrum of **IV** with $\mathbf{H}_0$ at setting A, under which conditions the parallel hfc feature of H^α is not present (data not shown). Diminution of the features for H^N is seen in the lower spectrum for a sample of **IV** dissolved in 8% [$^2H_6$]DMSO in ^2H_2O in which partial exchange of the amide proton with ^2H_2O has occurred. Although the exchange of H^N with solvent deuterons is expected to be kinetically facile, we have earlier observed that the exchange of H^N for spin-labeled phenylanine is significantly slower than for its methyl ester analogue.[11d] A similar phenomenon, as indicated in Figure 2, is observed for SLPheal.

In the upper spectrum of Figure 2, a prominent ENDOR feature is observed near the proton Larmor frequency with an approximate splitting of 0.11 MHz. Since we have observed the same 0.11 MHz resonance feature in the proton ENDOR spectrum of **IV** in a [^2H]chloroform/[$^2H_8$]toluene (50:50 v/v) cosolvent mixture containing 0.04 M [^2H]methanol, this feature must have its origin in the hemiacetal $-OCH_3$ group. The retention of these features in the upper spectrum thus indicates that the adduct formed through crystallization has not completely exchanged with bulk [$^2H_4$]methanol solvent under the conditions described in Figure 2. The resonance feature is similar to that of the ester CH_3O- group of methyl *N*-(2,2,5,5-tetramethyl-1-oxypyrrolinyl-3-carboxyl)-α-phenylalanate.[11d] On the other

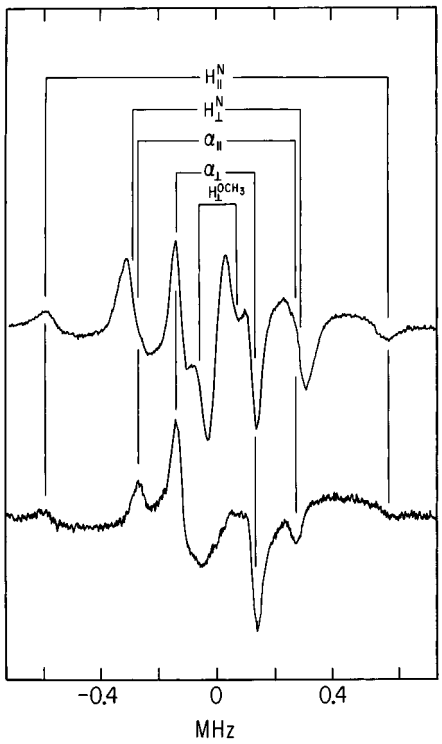

Figure 2. Proton ENDOR spectra of **IV** for setting B of the EPR spectrum. For each type of proton, two line pairs are seen symmetrically spaced about the proton Larmor frequency (14.33 MHz) and assigned to parallel and perpendicular hfc components. The abscissa indicates the ENDOR shift (measured ENDOR frequency minus free nuclear Larmor frequency). The ENDOR splittings are identified by stick diagrams for H^N, H^α, and H^{OCH_3}. The top spectrum was obtained from a solution of 3.0×10^{-3} M **IV** in [$^2H_6$]DMSO/[$^2H_4$]methanol (85:15 v/v), and the bottom spectrum was obtained from a solution of **IV** in 8% [$^2H_6$]DMSO, buffered to pD 7.0 with 0.025 M sodium cacodylate in 1.0 M NaCl.

hand, although the aldehyde is converted to the hydrated RCH-$(OH)_2$ species, the resonance features of the OH groups could not be detected separately from the broad matrix signal centered at the proton Larmor frequency.

Table 1 summarizes the principal hfc components of each proton assigned by specific deuteration and of the F^ζ substituent for the hydrated form of SLPheal in 8% [$^2H_6$]DMSO in ^2H_2O and for the hemiacetal derivative formed in neat methanol. Perpendicular hf couplings of H^α and H^{al} were readily assigned from ENDOR spectra of **IV** while the assignments of $H^{\beta1}$ and $H^{\beta2}$ were based on the spectra of **III**. There is overlap of resonance features for $H^{\beta1,2}$ similar to that observed for spin-labeled esters of aromatic amino acids.[11c,d] Proton ENDOR spectra of **V** were identical to those of **I** within the limits of spectral resolution. Therefore, the fluorine substituent has not altered the conformation of the spin-labeled aldehyde. For the hemiacetal adduct in neat perdeuterated methanol, inspection of the ENDOR spectra of **IV** after complete exchange of the hemiacetal $-OCH_3$ group revealed two sets of resonance features that could be assigned to H^{al} with distinguishably different electron−nucleus distances. We ascribe these to different positions of H^{al} with respect to the nitroxyl group for the hemiacetal adduct in *R* and *S* configurations which exist together in solution. The electron−nucleus separations estimated on the basis of the dipolar equation for each of these ENDOR active nuclei are also listed together in Table 1 with their corresponding line width based uncertainties. Within these uncertainties the overall conformation of the hemiacetal adduct of SLPheal in neat methanol is essentially identical to that of

TABLE 1: Summary of hfc Components (*A*, MHz) and Estimated Electron−Nucleus Distances (*r*, Å) of *N*-(2,2,5,5-Tetramethyl-1-oxypyrrolinyl-3-carboxyl)-L-phenylalaninal in 8% [$^2H_6$]DMSO in ^2H_2O and in [$^2H_4$]Methanol[a]

nucleus	$A_\parallel$	$A_\perp$	A_{iso}	$A_\parallel^D$	$A_\perp^D$	r^b
H^N	1.193	0.577	0.013	1.180	−0.590	5.12 ± 0.04
	1.190	0.577	0.012	1.178	−0.589	5.13 ± 0.06
H^α	0.542	0.262	0.006	0.536	−0.268	6.67 ± 0.10
	0.543	0.266	0.004	0.539	−0.270	6.66 ± 0.10
$H^{\beta1}$		0.190			−0.190	7.49 ± 0.12[c]
		0.195			−0.195	7.42 ± 0.10[c]
$H^{\beta2}$		0.130			−0.130	8.49 ± 0.20[c]
		0.140			−0.135	8.38 ± 0.25[c]
H^{al}	0.402	0.227	−0.017	0.419	−0.210	7.24 ± 0.10
	0.402	0.227	−0.017	0.419	−0.227	7.24 ± 0.30 (*R*)
	0.228	0.147	−0.002	0.286	−0.145	8.20 ± 0.30 (*S*)
F^ζ	0.245	0.135	−0.008	0.253	−0.127	8.38 ± 0.33
	0.255	0.139	−0.008	0.263	−0.131	8.28 ± 0.50
$-OCH_3$		0.092			−0.092	9.29 ± 0.30[d]

[a] The top row of values for each nucleus refers to the hydrated species of the spin-labeled inhibitor in aqueous solution. The lower row refers to the hemiacetal structure formed in neat methanol. [b] This laboratory has previously shown that the dipolar hfc components $A_\parallel^D$ and $A_\perp^D$ for nitroxyl spin-labels can be computed under the constraint $(A_\parallel + 2A_\perp) = 3A_{iso}$, where $A_\parallel$ and $A_\perp$ are the observed ENDOR splittings for the principal parallel and perpendicular hfc components, respectively, and $A_\parallel^D > 0 > A_\perp^D$.[11−13] On this basis, electron−nucleus distances can be directly calculated on the basis of the dipolar equation. Uncertainties in electron−nucleus distances are evaluated according to the line width of each absorption line. One-half of the full line width (ΔH_{pp}) between the extrema of the first-derivative curve was chosen as the uncertainty in transition frequency of an hfc component. This generally amounts to an uncertainty of 0.010−0.020 MHz. [c] The parallel hfc components of $H^{\beta1,2}$ could not be determined due to overlapping absorption lines. Therefore, the electron−nucleus distances of the two β protons were calculated on the basis of the observed perpendicular hfc components. As we have pointed out in the text, this approximation does not cause serious error because the isotropic hfc is negligible for these electron−nucleus separations. Similar overlap of resonances was observed for spin-labeled phenylalanine derivatives.[11d] [d] Refers to both *R* and *S* configurations of the hemiacetal adduct.

the hydrated species in aqueous solution while the relative disposition of groups bonded to the aldehydic C atom with sp^3 hydridization must differ for *R* and *S* configurations.

SLPheal Bound in the Active Site of αCT. ENDOR spectra of the enzyme:inhibitor adduct were taken under conditions of enzyme in excess, as described in Experimental Procedures, to ensure absence of overlapping contributions from free, unbound SLPheal in solution. In Figure 3 are illustrated ENDOR spectra of the hemiacetal adduct of αCT formed with SLPheal. The top spectrum is of **IV** bound to αCT while the lower spectrum is for the hemiacetal formed with **II**. As in the acylenzyme reaction intermediate formed with spin-labeled methyl L-tryptophanate,[12a] resonance features of $H^{\beta1,2}$ or protons of the aromatic side chain could not be identified. However, the perpendicular resonance features of H^α are identified through their absence in the spectrum of the inhibitor complex formed with **II** when compared to the upper spectrum. Similarly, the perpendicular ENDOR features for H^{al} are recognized in the spectrum of **II** when the overlapping features of H^α are removed through deuterium substitution.

Figure 4 compares the ^{19}F ENDOR spectra of the hemiacetal adduct of **V** formed with αCT with the spectra of **V** free in solution. While comparison of the spectra of the enzyme adduct to those of **V** free in solution shows that the hf couplings are distinguishably smaller for the enzyme-bound inhibitor than for the free inhibitor, we note that the parallel and perpendicular hfc components are more clearly resolved for the enzyme adduct

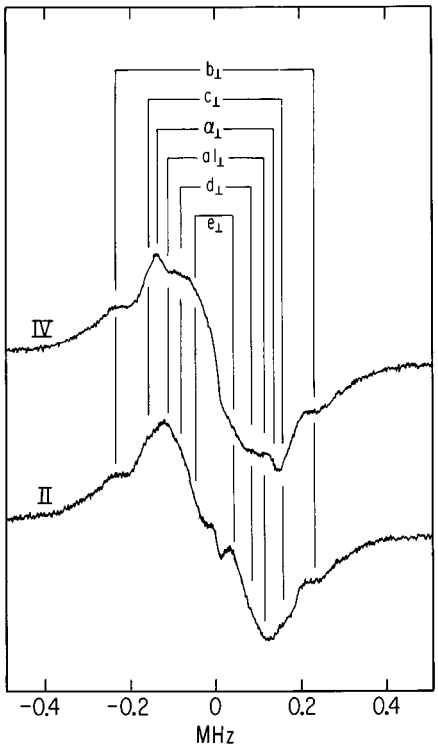

Figure 3. Proton ENDOR spectra of inhibitor adducts formed with αCT and SLPheal. The spectrum labeled **IV** is for the adduct of **IV** with αCT, and that labeled **II** is for the adduct of **II** with αCT. The static laboratory magnetic field was at setting A. Reaction conditions are as described under Experimental Procedures.

on the basis of $\mathbf{H}_0$ setting. These features are not as clearly resolved for the free inhibitor, as seen in the lower panel. The pattern of resonances for the enzyme-bound inhibitor requires that the ^{19}F substituent is positioned in the plane of the oxypyrrolinyl ring. This spectroscopic constraint for the enzyme-bound inhibitor acquires importance in structural modeling, as discussed later.

In Table 2, we have listed hf couplings and estimated dipolar electron−nucleus distances for H^{α}, H^{al}, and F^{ζ} in the enzyme−inhibitor adduct. The perpendicular hf coupling for H^{α} is seen to be slightly smaller than for the free inhibitor in aqueous DMSO. We also note that broad resonance features belonging to the protein and labeled H^a, H^b, H^c, H^d, and H^e were observed, comparable to those in the acylenzyme reaction intermediate of αCT,[12a] and their hf couplings are also summarized in Table 2. Although these resonance features cannot be assigned to specific enzyme residues, their corresponding "averaged" dipolar electron−proton distances are nearly identical to the values of *r* observed for clusters of active site residues in the spin-labeled tryptophanyl−αCT reaction intermediate.[12a]

Conformation of SLPheal Free in Solution and Bound in the Active Site of αCT. *SLPheal in Solution.* To determine the conformation of solvated SLPheal free in solution, we have carried out torsion angle search calculations within sterically allowed van der Waals space. Since ENDOR and NMR results indicated that SLPheal forms a hemiacetal adduct in methanol and a hydrated species in aqueous solutions, the aldehyde C atom was modeled as an sp^3 hybridized tetrahedral carbon atom rather than as the sp^2 carbon of an aldehyde group. In the enzyme:inhibitor adduct, it is expected that the aldehyde carbon is also converted to a tetrahedral center for hemiacetal formation.[7] The torsion angle search calculations were carried out generally in 5° increments for 0−360° rotation around the C(3)−C(6) and C(6)−N bonds within the spin-label acyl moiety and

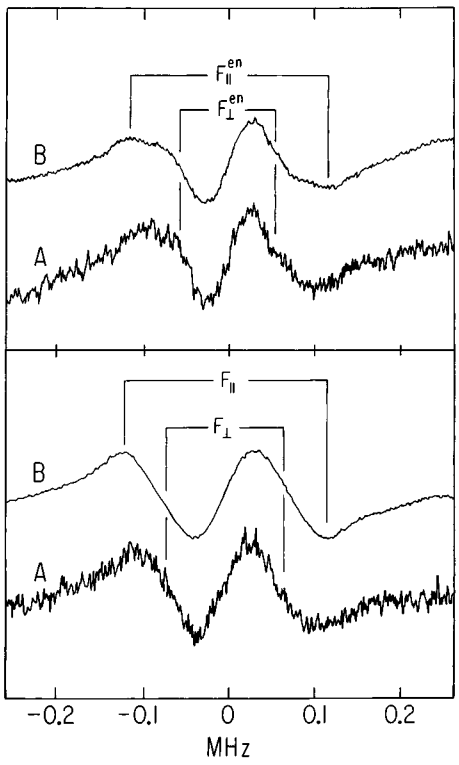

Figure 4. Fluorine-19 ENDOR spectra of **V** bound to αCT (top panel) and free in solution (lower panel) for $\mathbf{H}_0$ settings A and B. The spectra in the lower panel are for **V** in 8% [$^2H_6$]DMSO, as described in Figure 2, while the spectra in the upper panel are for **V** in the presence of αCT as described in Experimental Procedures. Resonance features are indicated in the stick diagrams in both top and bottom spectra and are labeled as $F_{\perp}$ and $F_{\parallel}$ for the free hydrated aldehyde of **V** and as $F_{\parallel}^{en}$ and $F_{\perp}^{en}$ for the adduct of **V** formed with αCT. Both $A_{\parallel}$ and $A_{\perp}$ of the free hydrated aldehyde of **V** are seen to be greater than for **V** complexed to αCT, indicating that the dipolar electron−nucleus distance in the free hydrated aldehyde of compound **V** is somewhat smaller than in the enzyme:SLPheal adduct.

TABLE 2: Summary of hfc Components (*A*, MHz) and Estimated Dipolar Distances (*r*, Å) for SLPheal and α-Chymotrypsin in the Enzyme:Inhibitor Adduct

nucleus	$A_{\parallel}$	$A_{\perp}$	r^a
inhibitor			
H^{α}		0.259	6.73 ± 0.2
H^{al}		0.223	7.10 ± 0.2
F^{ζ}	0.229	0.110	8.70 ± 0.4
enzyme[b]			
H^a	1.20	0.59	5.1 ± 0.1
H^b	0.90	0.47	5.6 ± 0.1
H^c		0.31	6.4 ± 0.2
H^d		0.16	7.9 ± 0.4
H^e		0.094	9.5 ± 0.6

[a] Electron−nucleus distances and associated uncertainties are evaluated as described in Table 1. [b] The categories of active site residues giving rise to these resonance features are listed as in the spin-labeled L-tryptophanyl-α-chymotrypsin reaction intermediate.[12a]

around the N−C^{α}, C^{α}−C, C^{α}−C^{β}, and C^{β}−C^{γ} bonds and the hemiacetal C−OCH_3 bond within the phenylalaninal moiety.

The structures of the hydrated aldehyde and of the hemiacetal adduct for both *R* and *S* configurations were compatible within van der Waals conformation space not only with the ENDOR determined distances listed in Table 1 but also with the constraint that the position of each ENDOR-active nucleus with respect to the magnetic axes defining the **g** matrix of the nitroxyl group was in agreement with its experimentally observed, angle-dependent hfc pattern. The results of the search calculations

TABLE 3: Comparison of Torsion Angles (in degrees) of the Reference Molecular Model and of the ENDOR-constrained Conformations of the Hydrate and Methanol Adducts of SLPheal

torsional angle	ref molec model	hydrate of SLPheal in 8% DMSO	SLPheal:CH_3OH hemiacetal adduct (*S*)[a]
[C(4)−C(3)−C(6)−N]	−31	−38 ± 10	−38 ± 13
[C(3)−C(6)−N−C^{α}]	−177	−175[b]	−175[b]
[C(6)−N−C^{α}−C]	−122	−120 ± 23	−98 ± 28
[N−C^{α}−C^{β}−C^{γ}]	−72	−63 ± 11	−62 ± 13
[C^{α}−C^{β}−C^{γ}−$C^{\delta 1}$]	96	90 ± 40	90 ± 40
[N−C^{α}−C−O_1]		−163 ± 15	−27 ± 15 (−53 ± 35)[c,d]
[N−C^{α}−C−O_2]		−75 ± 15	−95 ± 15 (−175 ± 35)[d,e]
[N−C^{α}−C−H^{al}]		−46 ± 15	−148 ± 15 (64 ± 35)
[C^{α}−C−O−CH_3]			165 ± 25 (−125 ± 75)[d,e]

[a] Results for the first five torsion angles listed below are essentially identical for both *R* and *S* configurations. The values of torsion angles within parentheses belong to the *R* configuration. [b] For simplification in the calculations, the value of this torsion angle was kept fixed as described in the text. [c] Corresponds to hemiacetal −OH. [d] The corresponding values for the reference molecular model are not indicated because they do not derive from X-ray-defined fragments but rather are constructed to impose sp^3 hybridization on the aldehydic C atom. [e] Corresponds to hemiacetal $-OCH_3$.

are listed in Table 3. As in our earlier studies of spin-labeled amino acids,[11b−d] we observed that the pseudo-peptide bond formed by acylation of the amine group exhibited, within narrow limits, a nearly exactly planar conformation on the basis of ENDOR distance constraints. For purposes of simplifying torsional angle search calculations, we consequently restricted the [C(3)−C(6)−N−C^{α}] torsion angle to −175°, at which value the number of calculated conformers accounted for most of the sterically accessible conformational space. Conformations involving the C atom of the hydrated species are defined on the basis of the electron−nucleus distance for H^{al} since resonances for the diol OH groups could not be identified. On the other hand, the resonance features of the hemiacetal $-OCH_3$ group could be identified, and the corresponding values of *r* for the geometrically averaged positions of the methyl protons were used for assignment of conformation for *R* and *S* configurations together with those for H^{al}.

Since two distinguishably different values of *r* for H^{al} were obtained for the hemiacetal adduct in methanol, we concluded that they belonged separately to the *R* and *S* configurations at the C atom. For simultaneous application of all distance constraints in the torsion angle search calculations, the *r* value of 7.24 ± 0.30 Å could be accommodated only by the *R* configuration while the *r* value of 8.20 ± 0.30 Å could be accommodated only by the *S* configuration. To test the correct assignment of values of *r* for H^{β},[1,2] the distances for $H^{\beta 1}$ and $H^{\beta 2}$ were switched. For both the diol species and the hemiacetal adducts, the calculated structures compatible with distance constraints were greatly reduced in number and showed eclipsed torsion angle relationships with respect to the C^{α}−C^{β} bond. Since such structural relationships must be associated with higher potential energy (and, therefore, lower population), they are not likely to represent the ground-state species in solution and were consequently discounted. In contrast to spin-labeled amino acids,[11b−d] equilibria involving multiple sets of conformations with respect to the conformation of the benzyl side chain were not identified.

Hemiacetal Enzyme:Inhibitor Adduct of SLPheal with αCT. The enzyme residues to define the active site were chosen by direct examination of the molecular model of tosyl αCT[4d] for which the solvent-accessible surface was calculated by the Lee−Richards algorithm.[24] The conformation of SLPheal bound in the active site of αCT was assigned according to ENDOR constraints as for free SLPheal in solution, except that the conformer search procedure was also restricted by the steric constraints of active site residues. The interaction of αCT with the inhibitor also supplied three further constraints to identify an ENDOR-compatible conformation of SLPheal in the tetrahedral adduct: (i) the aldehyde group of the inhibitor was constructed with a hemiacetal linkage so that the carbonyl carbon was positioned 1.43 Å from O^{γ} of Ser-195;[4d,9b] (ii) the aromatic side chain was positioned into the hydrophobic specificity pocket formed by residues 188−196, 212−221, and 226−228 similar to that found for the aromatic group in tosyl αCT[4d] and in the spin-labeled tryptophanyl acylenzyme species;[12a] and (iii) the aldehyde oxygen was positioned as an OH group with hydrogen bonding to backbone atoms of residues comprising the oxyanion hole.[4b,5] We specifically found that the hemiacetal OH could hydrogen bond to the carbonyl O of Cys-191, in addition to hydrogen-bonding interactions with other groups generally associated with the oxyanion hole.[5] The conformation of the spin-labeled phenylalaninal moiety in the active site of αCT was also defined by the ENDOR-determined electron−nucleus distances and hfc patterns dependent on $\mathbf{H}_0$ setting. For example, according to the hfc patterns in the upper panel of Figure 4, the F^{ζ} substituent must be located in the plane of the oxypyrrolinyl ring for the enzyme-bound inhibitor. Therefore, both the observed electron−fluorine distance and the position of the fluorine nucleus with respect to magnetic axes, as required by the resonance pattern in Figure 4, were applied as constraints to identify allowed conformers. *On this basis, the ENDOR constraints were compatible with only an* S *configuration of the aldehyde C atom for SLPheal in the active site as a tetrahedral adduct while the ENDOR results for the hemiacetal adduct of the inhibitor formed in neat methanol accommodated both* R *and* S *configurations.*

The conformation of the spin-labeled inhibitor bound in the active site of the enzyme as a tetrahedral hemiacetal adduct is shown in Figure 5. In this conformation the values of the torsion angles [C(4)−C(3)−C(6)−N], [C(3)−C(6)−N−C^{α}], and [C(6)−N−C^{α}−C] correspond closely to the those for the hydrated form of the free spin-labeled L-phenylalaninal. However, values of χ_1 and χ_2 in the hemiacetal adduct with αCT differ from those in the free inhibitor, resulting in a nearly eclipsed conformation of the side chain with respect to rotation around the C^{β}−C^{γ} bond. These relationships are more easily seen by comparison of the conformation of the free form of **V** in its *S* configuration with its enzyme-bound conformation in Figure 6. The conformation of SLPheal in the active site is essentially identical to that of the side chain of the spin-labeled tryptophanyl moiety in the acylenzyme reaction intermediate.[12a]

Discussion

Figure 6 compares the ENDOR determined structure of SLPheal as the free hemiacetal adduct formed with methanol and as the tetrahedral adduct in the active site of αCT. As seen in Figure 6, the conformation of the hemiacetal form of the free inhibitor with χ_1 and χ_2 values of −62° and 90°, respectively, is different from that in the tetrahedral adduct formed in the active site of αCT. This result, indicating that binding of the spin-labeled inhibitor into the active site requires a torsional alteration in structure, is consistent with our previous conclusions with respect to the difference in conformation of the spin-labeled L-tryptophan substrate free in solution and in the acylenzyme species of αCT.[12a] Furthermore, in our study of the acylenzyme reaction intermediate formed with the specific

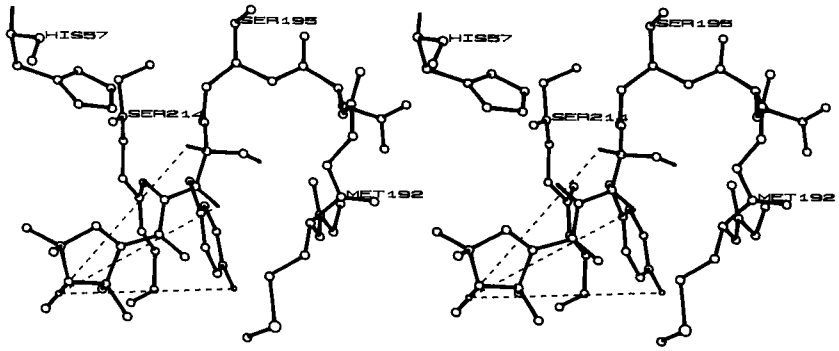

Figure 5. Stereodiagram of the hemiacetal of αCT with spin-labeled L-phenylalaninal in the active site. The conformation of the spin-labeled hemiacetal adduct is assigned on the basis of ENDOR determined electron−H^{α}, electron−H^{al}, and electron−F^{ζ} distances, illustrated by broken lines, and the requirement, as discussed in the text, that the F^{ζ} substituent of the side chain is coincident with the plane of the oxypyrrolinyl ring. These constraints applied collectively accommodate only an *S* configuration at the hemiacetal C atom.

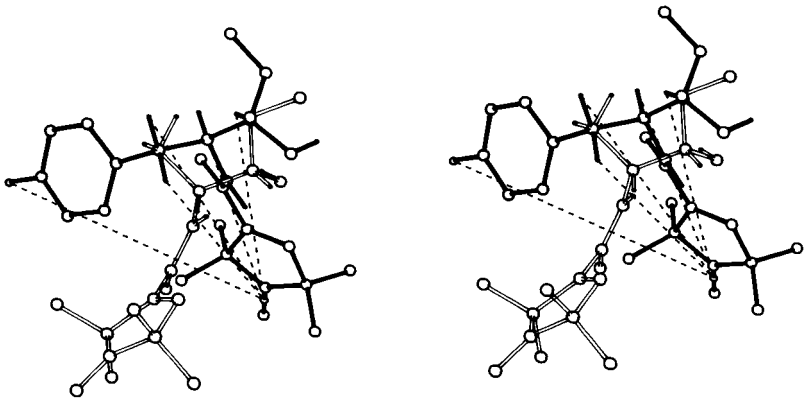

Figure 6. Stereodiagram comparing conformations of the hemiacetal form of compound **V** free in solution and in the active site of αCT. The two structures are compared by superposing the non-hydrogen atoms of the benzyl side chain of the phenylalaninal moiety. The free form of **V** is represented by solid bonds, and the electron−nucleus constraint distances to H^{α}, $H^{\beta,1,2}$ H^{al}, and F^{ζ} are illustrated by broken lines. The open bond structure corresponds to the enzyme-bound inhibitor superposed onto the solid bond structure of **V** free in solution. Through this diagram it is readily seen that in the enzyme-bound inhibitor the torsion angle χ_2 [$C^{\alpha}-C^{\beta}-C^{\gamma}-C^{\delta 1}$] is nearly eclipsed, similar to that in the spin-labeled tryptophanyl−αCT acylenzyme,[12a] in comparison to its essentially perpendicular conformation in the free inhibitor. While both *R* and *S* configurations were allowed for **V** free in solution, only the *S* configuration is illustrated here for direct comparison to the enzyme:inhibitor adduct.

spin-labeled ester substrate methyl *N*-(2,2,5,5-tetramethyl-1-oxypyrrolinyl-3-carboxyl)-L-tryptophanate,[12a] we detected five clusters of ENDOR resonance features from active side residues. In the present study we also observed five clusters of similar resonance features from enzyme residues with comparable hf couplings (cf. Table 2). The similar values of the hf couplings for the enzyme:inhibitor adduct and the acylenzyme reaction intermediate indicate that the location of the spin-label acyl moiety in the active site must be nearly identical with respect to these active site residues both in the inhibitor adduct and in the acylenzyme reaction intermediate. Thus, not only do the two types of spin-labeled amino acyl moieties exhibit similar conformations in the active site, but also the spin-labeled group is similarly positioned with respect to active site residues. This structural comparison of enzyme-bound substrate and inhibitor, based on spectroscopically determined hf couplings, provides the only evidence, to our knowledge, that aldehyde transition-state inhibitor analogues acquire conformations, when bound in the active site of αCT, that resemble those required for the catalytic conversion of substrate to product.

An important constraint in specifying the *S* configuration for the enzyme-bound inhibitor was the requirement that the predicted hfc pattern of the modeled structure remained compatible with experimental observation, in addition to application of only ENDOR determined electron−nucleus distances. Since the ENDOR determined hfc patterns of the enzyme:inhibitor adduct indicated that the protons and the fluorine atom were located in or very close to the plane of the oxypyrrolinyl ring (cf., Figure 4), this constraint was applied in molecular modeling. Although modeling of SLPheal into the active site of αCT showed that both *R* and *S* configurations of the hemiacetal adduct could be sterically accommodated, the inhibitor could not be modeled into the active site with an *R* configuration so as to satisfy both restrictions of hard-sphere interactions with enzyme residues and ENDOR constraints. The ENDOR determined distances to H^{al}, H^{α}, and the F^{ζ} substituent applied collectively, together with the constraint of locating the F^{ζ} substituent in the plane of the oxypyrrolinyl ring, excluded the *R* configuration unambiguously. In contrast, X-ray studies have shown that both *R* and *S* configurations were found in equal populations for the aldehyde peptide inhibitor chymostatin bound to protease A of *Streptomyces griseus*.[9b] In this enzyme it was concluded that the enzyme active site allowed approach of the aldehyde group so that the carbonyl O(H) was directed into the oxyanion hole or toward His-57. We believe that the more stringent discrimination of αCT for only one configuration is characteristic of the active site of αCT. It has been shown for a series of chiral aldehyde inhibitors that αCT exhibits greater discrimination in specificity of inhibitor binding in comparison, for instance, to the homologous bacterial enzyme subtilisin.[8]

On the basis of ENDOR characterization of the inhibitor dissolved in neat methanol, as outlined through results in Table 1 and Figure 2, it is evident that the aldehyde group of the

SCHEME 1

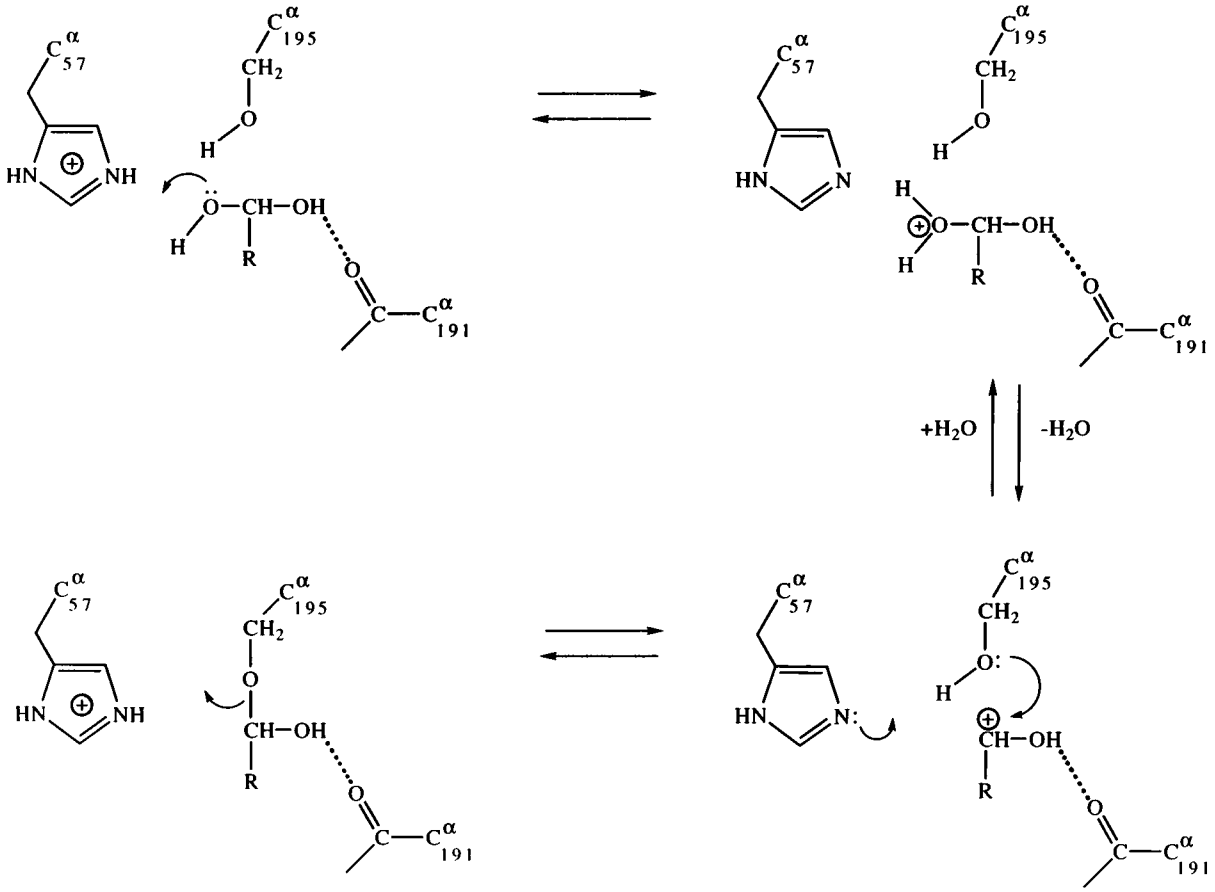

inhibitor readily enters into hemiacetal formation with an sp^3 hybridized carbon atom. In pure aqueous solution the $-$CHO group is expected to be predominantly converted to the achiral $-CH(OH)_2$ structure. It is, therefore, of some interest to consider the probable mechanism through which the hemiacetal enzyme:inhibitor adduct is formed with a resultant *S* configuration with total exclusion of the *R* configuration.

The conformation of an active site bound hydrated species is sterically restricted by (i) the side chain of Ser-195 preventing occupancy of that region by one of the OH groups and (ii) the tendency of an OH group to become hydrogen bonded with the carbonyl O of residue 191 and other residues forming the oxyanion hole. As outlined in Scheme 1, we suggest that His-57 in its protonated imidazolium form then catalyzes the dehydration of the diol through donation of its proton to the nearby OH group. This step, thus, mimics the reverse of the αCT catalyzed deacylation step in which a water molecule hydrogen bonded to $N^{\epsilon 2}$ (His-57) is activated to attack the carbonyl carbon of the acyl group.[4b,5] Because one OH group is stabilized in its position by residues of the oxyanion hole, dehydration results only in an *S* configuration because of steric constraints in the active site. Formation of a hemiacetal with an *R* configuration would require that upon binding of the diol species the OH group directed into the oxyanion hole be released through an acid-catalyzed process to allow adduct formation with the side chain of Ser-195. Since there is no nearby proton donor group in that region of the active site and the OH group can hydrogen bond to the carbonyl O of residue 191, it is stabilized in its position and is not released. The series of reactions depicted in Scheme 1 actually results in electrophilic catalysis to promote covalent bond formation with the O^{γ} of Ser-195 rather than only base-catalyzed nucleophilic attack of the serine side chain. Electrophilic catalysis would be expected to facilitate the reaction more than base-catalyzed nucleophilic attack since the partial charge on the carbonyl carbon is stabilized through both hydrogen bonding of the OH group in the oxyanion hole and loss of the other OH group as a neutral H_2O molecule. Scheme 1 is also consistent with the general observations that the hydrated species is readily converted to the free aldehyde by an acid-catalyzed process and that the role of His-57 is proton donation in the tetrahedral enzyme:substrate adduct to form an acylenzyme.[3,25]

It is of interest that Scheme 1 implies that binding of the diol form of an aldehyde may be more favorable to form a tetrahedral hemiacetal adduct than binding of the unhydrated aldehyde. In support of this notion, we note that the value of K_I for *trans*-cinnamaldehyde is 10-fold greater as a competitive inhibitor of αCT than is the value of K_I for hydrocinnamaldehyde. The latter is found predominantly in the hydrated form while less than 10% of *trans*-cinnamaldehyde is converted to a diol in aqueous solution.[26,27] Moreover, binding of the unhydrated aldehyde species would allow reactions that retard adduct formation with Ser-195. Henderson[4b] has suggested that stabilization of the acylenzyme of a nonspecific substrate could occur through bridging of a water molecule between $N^{\epsilon 2}$ (His-57) and the carbonyl O. A similar interaction with the carbonyl O of the (unhydrated) bound aldehyde is not likely to promote polarization of the carbonyl bond as strongly as interaction of the carbonyl O with residues defining the oxyanion hole. Furthermore, the hydrogen-bonded water molecule could become a nucleophile competing with hemiacetal formation by the side chain of Ser-195.

The tight steric demands of the catalytic triad and of the oxyanion hole in αCT allowing accommodation of only the *S*

configuration are consistent with the comparative enzymology of serine proteases. Protease A of *Streptomyces griseus*, which accommodates both *S* and *R* configurations of the inhibitor chymostatin as a hemiacetal adduct,[9] exhibits less substrate specificity than does αCT. Also, by comparison of the inhibitor binding constants for a series of chiral aldehyde[8] and boronic[28] acid inhibitor analogues of αCT and subtilisin Carlsberg, it has been demonstrated that αCT exhibits a greater power of discrimination toward chiral centers, in general. Thus, application of ENDOR spectroscopy to characterize active site structure results in a sensitive means for precise definition of stereochemical interactions between catalytic enzyme residues and reactive groups on the substrate. Comparable structural resolution cannot be achieved by other physical methods for molecules in solution.

Acknowledgment. We thank Dr. D. Mustafi for critical review of this manuscript and for helpful discussions. This research was supported by a grant of the National Institutes of Health (GM 21900).

References and Notes

(1) (a) Bender, M. L.; Kilheffer, J. V. *CRC Crit. Rev. Biochem.* **1973**, *1*, 149−199. (b) Bender, M. L.; Kezdy, F. J. *Annu. Rev. Biochem.* **1965**, *34*, 49−76.

(2) (a) Bender, M. L.; Kezdy, F. J. *J. Am. Chem. Soc.* **1964**, *86*, 3704−3714. (b) Bender, M. L.; Clement, G. E.; Gunter, C. R.; Kezdy, F. J. *J. Am. Chem. Soc.* **1964**, *86*, 3697−3703. (c) Zerner, B.; Bond, R. P. M.; Bender, M. L. *J. Am. Chem. Soc.* **1964**, *86*, 3674−3679.

(3) Hess, G. P. In *The Enzymes*; Boyer, P. D., Ed.; Academic Press: New York, 1971; Vol. 3, pp 213−248.

(4) (a) Steitz, T. A.; Henderson, R.; Blow, D. M. *J. Mol. Biol.* **1969**, *46*, 337−348. (b) Henderson, R. *J. Mol. Biol.* **1970**, *54*, 341−354. (c) Birktoft, J. J.; Blow, D. M.; Henderson, R.; Steitz, T. A. *Philos. Trans. R. Soc. London* **1970**, *B257*, 67−76. (d) Tsukada, H.; Blow, D. M. *J. Mol. Biol.* **1985**, *184*, 703−711.

(5) Blow, D. M. In *The Enzymes*; Boyer, P. D., Ed.; Academic Press: New York, 1971; Vol. 3, pp 185−248. (b) Blow, D. M. *Acc. Chem. Res.* **1976**, *9*, 145−151.

(6) Wolfenden, R. *Annu. Rev. Biophys. Bioeng.* **1976**, *5*, 271−306. (b) Thompson, R. C. *Biochemistry* **1973**, *12*, 47−51.

(7) (a) Chen, R.; Gorenstein, D. G.; Kennedy, W. P.; Lowe, G.; Nurse, D.; Schultz, R. M. *Biochemistry* **1979**, *18*, 921−926. (b) Lowe, G. O.; Nurse, D. *J. Chem. Soc., Chem. Commun.* **1977**, *22*, 815−817. (c) Wyeth, P.; Sharma, R. P.; Akhtar, M. *Eur. J. Biochem.* **1980**, *105*, 581−585.

(8) Lee, T.; Jones, J. B. *J. Am. Chem. Soc.* **1996**, *118*, 502−508.

(9) (a) James, M. N. G.; Sielecki, A. R.; Brayer, G. D.; Delbaere, L. T. J.; Bauer, C. A. *J. Mol. Biol.* **1980**, *144*, 43−88. (b) Delbaere, L. T.; Brayer, G. D. *J. Mol. Biol.* **1985**, *163*, 89−103.

(10) Abbreviations: αCT, α-chymotrypsin; DMSO, dimethyl sulfoxide; ENDOR, electron nuclear double resonance; hf, hyperfine; hfc, hyperfine coupling; rf, radio frequency; SLPheal, *N*-(2,2,5,5-tetramethyl-1-oxypyrrolinyl-3-carboxyl)-L-phenylalaninal.

(11) (a) Wells, G. B.; Makinen, M. W. *J. Am. Chem. Soc.* **1988**, *110*, 6343−6352. (b) Mustafi, D.; Sachleben, J. R.; Wells, G. B.; Makinen, M. W. *J. Am. Chem. Soc.* **1990**, *112*, 2558−2566. (c) Wells, G. B.; Mustafi, D.; Makinen, M. W. *J. Am. Chem. Soc.* **1990**, *112*, 2566−2574. (d) Joela, H.; Mustafi, D.; Fair, C. C.; Makinen, M. W. *J. Phys. Chem.* **1991**, *95*, 9135−9144. (e) Mustafi, D.; Joela, H.; Makinen, M. W. *J. Magn. Reson.* **1991**, *91*, 497−504.

(12) (a) Wells, G. B.; Mustafi, D.; Makinen, M. W. *J. Biol. Chem.* **1994**, *269*, 4577−4586. (b) Mustafi, D.; Makinen M. W. *J. Biol. Chem.* **1994**, *269*, 4587−4595.

(13) Makinen, M. W.; Mustafi, D.; Kasa, S. In *Biological Magnetic Resonance. Spin-Labeling: The Next Millenium;* Berliner, L. J., Ed.; Plenum Publishing: New York, 1997; Vol. 14, in press.

(14) Ito, A.; Tamahashi, R.; Baba, Y. *Chem. Pharm. Bull.* **1975**, *23*, 3081−3087.

(15) Churg, A. K.; Gibson, G.; Makinen, M. W. *Rev. Sci. Instrum.* **1978**, *49*, 212−214.

(16) Wells, G. B. Ph.D. Thesis, The University of Chicago, Chicago, IL, 1987.

(17) Maret, W.; Makinen, M. W. *J. Biol. Chem.* **1991**, *266*, 20636−20644.

(18) Dixon, M.; Webb, E. C. *The Enzymes*, 2nd ed; Academic Press: New York, 1964; p 327.

(19) Jiang, F. S.; Makinen, M. W. *Inorg. Chem.* **1995**, *34*, 1736−1744.

(20) (a) Jones, T. A. *Methods Enzymol.* **1985**, *115*, 147−171. (b) Dayringer, H. E.; Tramontano, A.; Sprang, S. R.; Fletterick, R. J. *J. Mol. Graphics* **1984**, *4*, 82−87. (c) Marshall, G. R., personal communication. (d) Detailed information on the use of the program package SYBYL can be obtained from Tripos Associates, Inc., 1600 S. Hanley Road, St. Louis, MO 63144.

(21) Iijima, H.; Dunbar, J. B., Jr.; Marshall, G. R. *Proteins: Struct. Funct. Genet.* **1987**, *2*, 330−339.

(22) Naruto, S.; Motoc, J.; Marshall, G. R.; Daniels, S. B.; Sofia, M. J.; Katzenellenbogen, J. A. *J. Am. Chem. Soc.* **1985**, *107*, 5262−5270.

(23) Kennedy, W. P.; Schultz, R. M. *Biochemistry* **1979**, *18*, 349−356.

(24) Lee, B.; Richards, F. M. *J. Mol. Biol.* **1971**, *36*, 85−90.

(25) Liang, T. C.; Abeles, R. H. *Biochemistry* **1987**, *26*, 7603−7608.

(26) Rawn, J. D.; Lienhard, G. E. *Biochemistry* **1974**, *13*, 3124−3131.

(27) Bell, R. P. *Adv. Phys. Org. Chem.* **1966**, *4*, 1−29.

(28) Martichonok, V.; Jones, J. B. *J. Am. Chem. Soc.* **1996**, *118*, 950−958.